ResearchGate

See discussions, stats, and author profiles for this publication at: https://www.researchgate.net/publication/226285097

Impurity radiation from a tokamak plasma

Article *in* Plasma Physics Reports · January 2007

DOI: 10.1134/S1063780X07110037

CITATIONS
17

READS
441

3 authors, including:

Elena Olegovna Baronova
Kurchatov Institute
71 PUBLICATIONS **211** CITATIONS
SEE PROFILE

Ilya Senichenkov
Peter the Great St.Petersburg Polytechnic University
47 PUBLICATIONS **450** CITATIONS
SEE PROFILE

Some of the authors of this publication are also working on these related projects:

carbon dioxide reduction View project

Comparing N vs Ne as divertor radiators for tokamak plasmas with SOLPS-ITER modeling View project

All content following this page was uploaded by Elena Olegovna Baronova on 02 February 2016.

The user has requested enhancement of the downloaded file.

ISSN 1063-780X, Plasma Physics Reports, 2007, Vol. 33, No. 11, pp. 906–922. © Pleiades Publishing, Ltd., 2007.
Original Russian Text © D.Kh. Morozov, E.O. Baronova, I.Yu. Senichenkov, 2007, published in Fizika Plazmy, 2007, Vol. 33, No. 11, pp. 988–1005.

PLASMA
RADIATION

Impurity Radiation from a Tokamak Plasma

D. Kh. Morozov[a], E. O. Baronova[a], and I. Yu. Senichenkov[b]

[a] *Nuclear Fusion Institute, Russian Research Centre Kurchatov Institute, pl. Kurchatova 1, Moscow, 123182 Russia*
[b] *St. Petersburg State Polytechnical University, Politekhnicheskaya ul. 29, St. Petersburg, 195251 Russia*

Received November 24, 2006; in final form, February 20, 2007

Abstract—In tokamak operating modes, energy balance is often governed by impurity radiation. This is the case near the divertor plates, during impurity pellet injection, during controlled discharge disruptions, etc. The calculation of impurity radiation is a fairly involved task (it is sometimes the most difficult part of the general problem) because the radiation power is determined by the distribution of ions over the excited states and by the rate constants of elementary processes of radiation and absorption. The objective of this paper is to summarize in one place all the approximate formulas that would help investigators to describe radiation from the most often encountered impurities in a fairly simple way in their calculations accounting for plasma radiation, without reference to special literature. Simple approximating formulas describing ionization, recombination, and charge-exchange processes, as well as radiative losses from ions with a given charge, are presented for five impurity species: beryllium, carbon, oxygen, neon, and argon. Estimating formulas that allow one to take into account plasma opacity for resonant photons in line impurity radiation are also presented.

PACS numbers: 52.25.Vy, 52.25.Os

DOI: 10.1134/S1063780X07110037

1. INTRODUCTION

Impurity radiation has a substantial effect on the energy balance and, consequently, on the dynamics of plasma parameters in many processes in tokamak plasmas, e.g., in the current decay process after a major disruption [1] and in the processes occurring after the injection of a neutral gas jet in order to prevent catastrophic consequences during major disruptions or forced power cuts [2–5]. In such circumstances, the plasma is often opaque to photons in line impurity radiation [6]. Recipes for calculating radiative losses have been developed and published long ago (see, e.g., [7, 8]), but their direct application runs into certain difficulties. In fact, when all the densities n_z of the ions with a charge number z are known, the radiation intensity Q_z from an impurity of a given species in an optically thin plasma can be calculated from the formula

$$Q_z = n_e \sum n_z L_z(T_e). \quad (1.1)$$

This formula is valid under the following assumptions: the characteristic ionization and recombination times are longer than the times of natural radiative decay of the excited states, the plasma density is such that the mixing of the neighboring levels is unimportant, the electromagnetic fields do not allow forbidden lines to be emitted, etc. If these assumptions, or some of them, are not satisfied, then it is necessary to construct a complete radiative–collisional model in which the deviation of the electron distribution function from being Maxwellian should generally be taken into account.

The relative radiation intensity $L_z(T_e)$ is contributed by the bremsstrahlung and recombination radiation in the continuum and by the line radiation. The spectra have very many lines, and formulas for determining the line intensities are rather complicated. This is why the calculation of the relative radiation intensity $L_z(T_e)$ is a fairly laborious procedure, which is especially involved when it is necessary to account for opacity effects. In this case, the plasma is very far from being in a coronal equilibrium state or in a locally thermodynamic equilibrium state. This fact does not complicate calculations in zero- and one-dimensional models, but as for two- and three-dimensional self-consistent simulations with allowance for radiation, they cannot be carried out on personal computers.

On the other hand, direct calculations show that the function $L_z(T_e)$ can often be approximated with a good accuracy by a spectrum having a small number of lines with the effective transition energies E_z^{jk} and oscillator strengths f_z^{jk} and that the opacity effects can be accounted for by simple estimating expressions when the excited levels are far less populated than the ground state. Moreover, for some impurities in an optically thin plasma, approximating expressions are very simple, so impurity radiation can be easily incorporated in the energy balance, the amount of calculations can be greatly reduced, and some qualitative results can be obtained analytically.

Similar difficulties arise in calculating the dielectronic recombination rate.

The goal of the present paper is to propose a reasonable simplifying algorithm for calculating impurity radiation. This algorithm can be used (along with various models of the time evolution of the plasma) to calculate the intensities of line emission from the plasma and the corresponding radiative losses. When applied to multidimensional MHD models, the approach proposed here will considerably reduce the computer time and provide more correct and realistic predictions of the behavior of the main plasma parameters. Unfortunately, the algorithm for estimating radiation is not universal and should be adjusted for each particular plasma. The proposed model should be verified by a comparison with the measured radiative and other plasma parameters (e.g., the spectra, radiative losses, electron velocity distributions, etc.). Any model requires such testing because, on the one hand, the main criterion for the proposed model to be correct is that the calculated results coincide with the experimental data and, on the other hand, a search for reasons why numerical results differ from the measured ones can substantially improve the model or reveal inaccuracies in experiments.

In what follows, we present simplified expressions for the radiation intensity from individual ions in an optically thin plasma. We combine the numerous emission lines into several groups, each characterized by its effective oscillator strength and transition energy.

Since the mean free path of a resonant photon depends strongly on the wavelength, the spectral line resulting from radiative losses in an optically thin plasma can be appreciably suppressed in an optically thick plasma. Consequently, elementary approximating formulas accounting only for the most intense emission lines from an optically thin plasma fail to hold for an optically thick plasma. However, numerous lines can be combined into several (no more than six) groups with close wavelengths and, accordingly, with close absorption coefficients. We will present the effective transition energies and oscillator strengths for such groups. We also write out formulas accounting for the opacity effects for each of the groups and give the values of the parameters in the formulas.

In addition, we present elementary formulas approximating the dielectronic recombination rate and describing the results of "exact" calculations (i.e., those from the complicated expressions of quantum mechanics) with an accuracy of no worse than 25% over the temperature and density ranges characteristic of the processes occurring in tokamaks.

For reference, we also give simple formulas for bremsstrahlung and recombination radiation from handbooks. We also write out formulas for electron impact ionization rates, charge exchange, three-body recombination, and photorecombination and present the constants required for calculations.

For convenience, the Appendix lists the notation used in this paper.

2. IMPURITY RADIATION

The energy associated with impurity radiation is lost through three channels: line emission, bremsstrahlung, and recombination radiation.

In all the formulas presented below, the temperature and transition energies are expressed in electronvolts.

Recombination radiation and bremsstrahlung have been studied in many papers (see, e.g., [8, 9]). This research yielded the following simple approximating formulas, which can be found, e.g., in [10]: $L_{\mathrm{Rr}}^z = 1.69\times10^{-25}\sqrt{T_e}\,z^2\left(\frac{E_{\mathrm{ion}}^{z-1}}{T_e}\right)$ erg cm^3/s for recombination radiation and $L_{\mathrm{Br}}^z = 1.69\times10^{-25}\sqrt{T_e}\,z^2$ erg cm^3/s for ion bremsstrahlung, where z is the charge number of an ion and E_{ion}^{z-1} is the ionization energy of a recombination-produced ion. The formula for bremsstrahlung ignores the fact that high-energy electrons can penetrate into the electron shell of a slightly stripped ion, so, generally speaking, it is necessary to introduce an effective charge into the formula. However, since slightly stripped ions radiate predominantly in lines, this effect can be ignored in calculating radiative losses.

The calculation of the intensity of line radiation is more complicated task. The physics of this radiation is described in sufficient detail in reviews [9, 11, 12] and also in [13]. For an optically thin plasma, the populations of the excited levels can be assumed to be low in comparison with that of the ground state. It can also be assumed that the radiation process occurs in the following way: an ion is excited into a higher level by electron impact to immediately emit a photon with an energy equal to the transition energy. Accordingly, the intensity of an emission line is calculated as the product of the electron-impact excitation rate and the transition energy [7, 9] with allowance for transitions of only valence electrons to the excited levels.

For transitions in which the principal quantum number does not change ($n_1 - n_0 = 0$, where n_0 and n_1 are the principal quantum numbers of the initial and final states, respectively), the intensity of a given emission line is described by the expression

$$L_z^j = 2.5\times10^{-17}\frac{f_z^{0j}}{\sqrt{T_e}}A_1^z(E_z^{0j})\ \text{erg/cm}^3\text{/s}, \qquad (2.1)$$

where

$$A_1^z = \begin{cases} 0.06\dfrac{\sqrt{\dfrac{E_z^{0j}}{T_e}} - 2}{1 + \dfrac{E_z^{0j}}{T_e}} \exp\left(-\dfrac{E_z^{0j}}{T_e}\right) + 0.276E_1\left(\dfrac{E_z^{0j}}{T_e}\right), \\ \text{for } z = 0 \text{ (neutrals)}, \\ a_n \exp\left(-\dfrac{E_z^{0j}}{T_e}\right) + 0.276E_1\left(\dfrac{E_z^{0j}}{T_e}\right), \\ \text{for } z \neq 0, \end{cases} \quad (2.2)$$

E_z^{0j} is the energy of a transition from the ground state to the jth excited state, and $E_1(x) = \int_x^\infty \dfrac{\exp(-t)dt}{t}$ is the integral exponent. To within an accuracy of 1.5%, the integral exponent can be calculated from the following simple approximating formula, which yields a correct asymptotic and a correct series expansion:

$$E_1(x) \approx \begin{cases} -0.5772 - \ln x + 0.80x^{0.85} \text{ for } x \leq 1, \\ \dfrac{\exp(-x)}{x}\dfrac{x + 0.5}{x + 1.5} \text{ for } x > 1. \end{cases} \quad (2.3)$$

In formula (2.2), the coefficients $a_n \equiv d_{nn}\left(1 - \dfrac{\gamma_{nn}}{z}\right)$ are expressed in terms of the constants presented in [7].

For transitions in which the principal quantum number changes, $n_1 - n_0 \neq 0$, we have

$$L_z^j = 4.8 \times 10^{-18} \frac{f_z^{0j}}{\sqrt{T_e}} A_2^z \text{ erg/cm}^3\text{/s}, \quad (2.4)$$

where

$$A_2^z = \exp\left(-\frac{E_z^{0j}}{T_e}\right) + 0.9\left(1 + \frac{n_1(n_1 - n_0)}{20} \times \left(1 + \frac{Z - 2}{Z}\frac{E_z^{0j}}{T_e}\right)\right)E_1\left(\frac{E_z^{0j}}{T_e}\right), \quad (2.5)$$

and Z is the nuclear charge. Expressions (2.1)–(2.5) can be obtained from the formulas of [7] by simple redefinitions.

The tokamak plasma is almost always transparent to bremsstrahlung and recombination radiation. The situation with line radiation is radically different. In some cases, such as the diagnostic pellet injection or the injection of noble gas jets (to reduce the consequences of major disruptions), as well as the current decay process after a major disruption (when a large amount of impurities come from construction materials), the plasma becomes partially or even completely opaque to line radiation. A photon emitted by an ion in the radiative decay of an excited state is a resonant one for an ion with the same charge. The mean distance that such a resonant photon travels before being absorbed can be less than the characteristic dimension of a cloud of ions of a given species, $\kappa_z^j \rho \leq 1$, where κ_z^j is the reciprocal of the photon mean free path and ρ is the characteristic dimension of the ion cloud. The resonant photon may then suffer three fates.

When walking between the ions, an excited ion may occur near enough to the cloud boundary for the photon emitted in a radiative decay event to escape from the cloud. Note that the cloud boundary does not necessarily coincide with the plasma boundary: e.g., radiation emitted from a triply charged ion passes freely through the surrounding cloud of lower charged ions.

The wavelength of the photon can change, in particular, due to the Doppler effect; in this case, the photon becomes nonresonant and also escapes from the cloud.

The excited state of an ion is quenched by electron impact, so the photon energy falls into the electron continuum.

The attenuation of radiation emitted in a given line from a plane ion slab can be approximately accounted for by the factor

$$B_z^j = \frac{1}{1 + \beta_z^j} W_z^j, \quad (2.6)$$

Here, the parameter

$$\beta_z^j = \frac{2.7 \times 10^{-13} n_e}{(E_z^{0j})^3 \sqrt{T_e}}\left[1 - \frac{E_z^{0j}}{T_e}\exp\left(\frac{E_z^{0j}}{T_e}\right)E_1\left(\frac{E_z^{0j}}{T_e}\right)\right] \quad (2.7)$$

is the ratio of the electron-impact quenching probability to the radiative decay probability [14] and the function W_z^j, describing the plasma opacity, has the form

$$W_z^j = \frac{(1 + \beta_z^j)T_a}{\beta_z^j + T_a}, \quad (2.8)$$

where T_a is the probability for a photon to travel a distance ρ without being absorbed. For a Doppler-broadened line in the case $\kappa_z^j \rho \gg 1$, we can set [15]

$$T_a = (\kappa_z^j \rho \sqrt{\pi \ln(\kappa_z^j \rho)})^{-1}. \quad (2.9)$$

This expression diverges for infinitely thin ion clouds. The divergence can be eliminated by using the approximating formula

$$T_a = (1 + \kappa_z^j \rho \sqrt{\pi \ln(\kappa_z^j \rho + 1)})^{-1}. \quad (2.10)$$

Finally, we have

$$B_z^j = (\beta_z^j(1 + \kappa_z^j \rho \sqrt{\pi \ln(\kappa_z^j \rho + 1)}) + 1)^{-1}. \quad (2.11)$$

The reciprocal of the photon mean free path is described by the relationship [14]

$$\kappa_z^j = \frac{n_z(\lambda_z^j)^2}{4\pi}\frac{1}{1+\Gamma/\gamma}, \quad (2.12)$$

where λ_z^j is the photon wavelength and Γ/γ is the ratio between the observed and natural (radiative) line widths. For a Doppler-broadened line, we have

$$\kappa_z^j = \frac{n_z(\lambda_z^j)^2}{4\pi}\frac{1}{1+1.11\times10^{10}E_z^{0j}\sqrt{\frac{m_p}{M}T_e}/\nu_z^j}, \quad (2.13)$$

where ν_z^j is the reciprocal of the natural radiative decay time of an excited state, m_p is the mass of a proton, and M is the mass of an ion.

For an optically thick plasma, radiation should generally be calculated with allowance for transitions between the excited states. However, in many important cases, such transitions can be ignored.

3. IONIZATION, RECOMBINATION, AND CHARGE EXCHANGE

The rates of all the processes considered below correspond to a Maxwellian electron distribution and are expressed in cm^3/s.

For an optically thin plasma, the ionization rate can be calculated with allowance for only electron-impact ionization from the ground state [10]:

$$I_{z\text{ground}} = 10^{-5}\frac{\sqrt{T_e/E_{\text{ion}}^z}}{(E_{\text{ion}}^z)^{3/2}(6.0+T_e/E_{\text{ion}}^z)}\times\exp(-E_{\text{ion}}^z/T_e). \quad (3.1)$$

For an optically thick plasma with a temperature lower than the energy of ionization from the ground state, it is necessary to take into account ionization from an excited state, although the excited level can be still far less populated than the ground state. In this case, the rate of ionization from an excited state is described by the expression [16, 17]

$$U_{z\text{ex}} = \frac{3.27\times10^{-5}}{(T_e)^3}\exp\left(-\frac{E_{\text{ion}}^z}{T_e}\right). \quad (3.2)$$

Expression (3.2) was derived under the assumption that the population of the excited levels obeys a Boltzmann distribution. This assumption is valid for $\beta_z^j \gg 1$, i.e., when electron-impact quenching predominates over the radiative decay of the excited states. For low electron densities, this assumption fails to hold, so formula (3.2) cannot be used under the conditions of the coronal model. Unfortunately, we do not know a simple expression describing ionization from the excited state for arbitrary electron densities.

The total ionization rate is described by the expression

$$I_z = I_{z\text{ground}} + I_{z\text{ex}}. \quad (3.3)$$

The three processes that take part in recombination are known to be three-body recombination; photorecombination; and dielectronic recombination, which occurs when the recombining ion has at least one electron. The dielectronic recombination is in essence a kind of photorecombination, when several (rather than one) photons are emitted.

The three-body recombination is important only at high densities and low temperatures; its rate is given by the formula [10]

$$R_{3b}^z = 8.75\times10^{-27}z^3n_eT_e^{-9/2}. \quad (3.4)$$

The expression for the photorecombination rate has the form [8]

$$R_{\text{photo}}^z = 5.2\times10^{-14}z\sqrt{\frac{E_{\text{ion}}^{z-1}}{T_e}}\times\left(0.43+0.5\ln\frac{E_{\text{ion}}^{z-1}}{T_e}+0.469\left(\frac{E_{\text{ion}}^{z-1}}{T_e}\right)^{-1/3}\right). \quad (3.5)$$

In the most general case, the dielectronic recombination is the sum of rates over all possible transitions in the electron shell of a recombining ion [7, 18]:

$$R_{\text{diel}}^z = B_z\sum_j A_{zj}D_{zj}\frac{\exp(-E_z^{0j}/T_e)}{T_e^{3/2}}, \quad (3.6)$$

$$B_z = 6.5\times10^{-10}(z+1)^2\sqrt{\frac{z}{z^2+\text{Ry}}}, \quad (3.7)$$

$$A_{zj} = \frac{f_z^{0j}\sqrt{E_z^{0j}}}{1+0.105a_z^j+0.015a_z^{j^2}}, \text{ for } n_1-n_0=0, \quad (3.8)$$

$$A_{zj} = \frac{0.5f_z^{0j}\sqrt{E_z^{0j}}}{1+0.21a_z^j+0.03a_z^{j^2}}, \text{ for } n_1-n_0\neq0, \quad (3.9)$$

$$a_z^j = E_z^{0j}/((z+1)Ry), \quad (3.10)$$

$$D_{zj} = \frac{n_t/200}{1+n_t/200}, \text{ for } n_1-n_0=0, \quad (3.11)$$

$$D_{zj} = \frac{0.0015((z+1)n_t)^2}{1+0.0015((z+1)n_t)^2}, \text{ for } n_1-n_0\neq0, \quad (3.12)$$

$$n_t = \left(\frac{4.77\times10^{18}}{\sqrt{1000}}z^6\frac{\sqrt{T_e}}{n_e}\right)^{1/7}, \quad (3.13)$$

Here, z is the charge number of a recombining ion and Ry = 13.4.

Energy losses are substantially influenced by the charge exchange of impurity ions with neutral hydrogen, which can penetrate from the wall deep into a tokamak discharge plasma. The cross section for charge exchange of the ions with neutral atoms was thoroughly studied both theoretically and experimentally (see, e.g., [19]). For relative velocities much lower than the Bohr orbital velocity in a hydrogen atom, a simple analytic formula for the charge-exchange cross section was obtained by Chibisov [20]. In a later paper by Phaneuf et al. [21], an empirical expression was presented that describes the cross section for charge exchange between an ion with a charge number z and a neutral hydrogen atom in the ground state and fits well with the experimental data over a broad energy range:

$$\sigma_z^{\rm cx} = \frac{5.967\times10^{-17} z \ln\left(\frac{5.87\times10^5\sqrt{z}}{E_n}\right)}{1 + 1.913\times10^{-3}E_n^2/z + 1.383\times10^{-7}(E_n\sqrt{z})^{9/2}}\ {\rm cm}^2, \quad (3.14)$$

where E_n is the kinetic energy of a hydrogen atom. In the temperature range $T_e \le 30$ eV, the charge-exchange rate corresponding to expression (3.14) for a Maxwellian distribution of hydrogen atoms is well approximated by a very simple formula,

$$R_{\rm cx} = \langle \sigma_{\rm cx} v\rangle \approx 3.5\times10^{-10} z(\sqrt{T_n} + 1.5)\ {\rm cm}^3/{\rm s}, \quad (3.15)$$

where T_n is the neutral hydrogen temperature. Accounting for charge exchange of ions with atoms in the excited states may increase the charge-exchange cross section severalfold [22, 23]. However, calculation of the occupation numbers of the excited levels is a separate, rather complicated problem.

For some many-electron ions, the ionization energy is lower than that for a hydrogen atom. For example, the ionization energy of neutral carbon is equal to 11.26 eV, while that of hydrogen is 13.6 eV. Obviously, the rate of charge exchange of C^+ ions with neutral hydrogen should decrease abruptly in the range $T_n < 2.34$ eV. This circumstance, which is ignored in formulas (3.14) and (3.15), can be roughly taken into account by equating the charge-exchange rate of the corresponding ion to zero for temperatures below the difference between the ionization energies.

4. APPROXIMATIONS

In this section, we list the approximations for the radiation intensities in a six-group model, the approximating expressions for the intensity of radiation from an optically thin plasma, and the approximations for the dielectronic recombination rate. We also give the deviations of the approximate results from the results of exact calculations. For carbon radiation in an optically thin plasma, similar approximating formulas are presented in [24]. In the exact calculations, all the emission lines for which $f_z^{jk} \ge 10^{-2}$ were taken into account [25]. The radiation intensity was calculated from formulas (2.1)–(2.3); the corrections for the opacity effects, from formulas (2.8), (2.9), (2.12), and (2.14); and the exact dielectronic recombination rate, from formulas (3.6)–(3.13). Note that the approximating formulas for dielectronic recombination were obtained for the temperature range in which, on the one hand, $R_{\rm diel}^z \ge R_{\rm photo}$ (for lower temperatures, the proposed approximations underestimate the dielectronic recombination rate—a circumstance that is, however, unimportant because the ratio of this rate to the photorecombination one decreases very sharply with temperature) and, on the other hand, the ionization rate is more than four orders of magnitude slower than the dielectronic recombination rate. In the opposite case, either the density of the ions with a given charge number is negligibly low or the recombination in dynamic processes can be ignored.

The intensity of radiation from an ion with a charge number z in an optically thin plasma can be described by the formula

$$L_z = \sum_j L_z^j \approx 10^{-18} T_e^{-\lambda}\left(C_1^{\rm rad}\exp\left(-\frac{E_1^{\rm rad}}{T_e}\right) + C_2^{\rm rad}\exp\left(\frac{-E_2^{\rm rad}}{T_e}\right)\right)\ {\rm erg\ cm^3/s}. \quad (4.1)$$

The values of the parameters $C_{1,2}^{\rm rad}$, $E_{1,2}^{\rm rad}$, and λ are given in the tables.

The dielectronic recombination rate is well approximated by the formula

$$R_{\rm diel} \approx 10^{-9}\left(C_z^1\exp\left(-\frac{E_{\rm dr}^{(1)}}{T_e}\right)\left(\frac{n_e}{N}\right)^{-\beta_1} + C_z^2\exp\left(-\frac{E_{\rm dr}^{(2)}}{T_e}\right)\left(\frac{n_e}{N}\right)^{-\beta_2}\right)T_e^{-\alpha}\ {\rm cm}^3/{\rm s}. \quad (4.2)$$

This formula is valid for all impurities over the entire range of temperatures at which dielectronic recombination is important but which are lower than 10^4 eV. For higher temperatures, the accuracy of formula (4.2) has not been examined. In this formula, $N = 10^{12}$ cm^{-3}. The

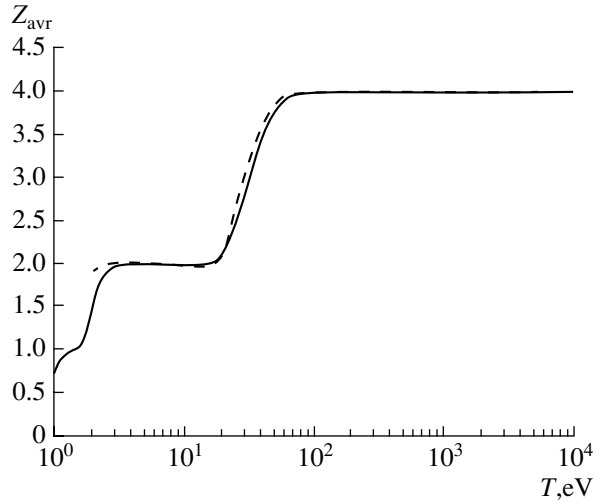

Fig. 1. Charge number of beryllium, averaged over the ionization states, vs. temperature in a coronal equilibrium. The solid curve shows the results of calculations by the model proposed in the present paper, and the dashed curve shows the results of Post et al. [7].

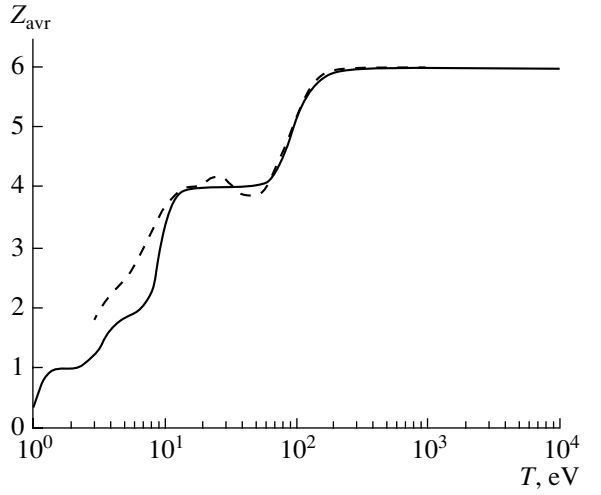

Fig. 2. The same as in Fig. 1, but for carbon.

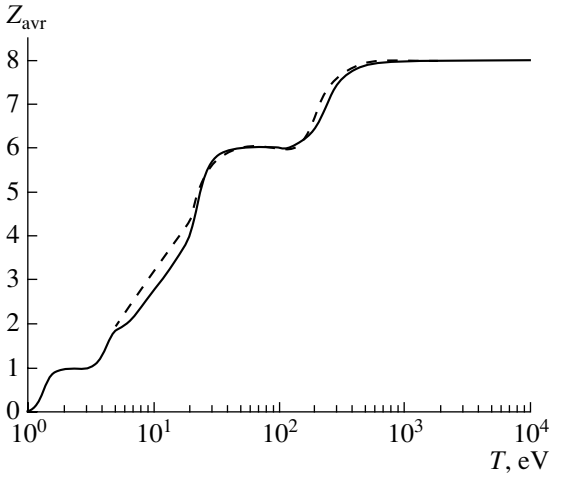

Fig. 3. The same as in Fig. 1, but for oxygen.

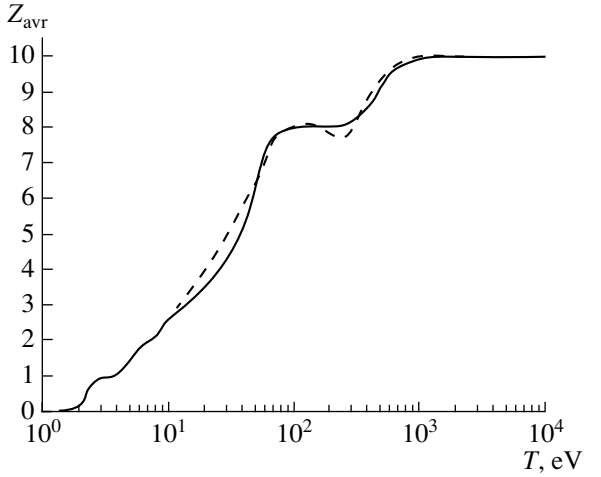

Fig. 4. The same as in Fig. 1, but for neon.

parameters $C_z^{1,2}$, C_z^2, β_1, β_2, and α, as well as the effective values of the energies $E_{dr}^{1,2}$, are presented in the tables, which also give the percent deviations Δ_{er} of the approximating formula from the exact one in the density range 10^{12} cm$^{-3} \le T_e \le 10^{17}$ cm^{-3}.

5. COMPARISON WITH THE KNOWN RESULTS FOR AN OPTICALLY THIN PLASMA

In order to check the applicability of the model proposed here, we compared the results of our model calculations of the ion charge averaged over the ionization states and of the specific power of radiation from all the five impurities in coronal equilibrium with the previous results [7, 26]. The temperature dependence of the average charge number is shown in Figs. 1–5. The dielectronic recombination rate was calculated for an electron density of 10^{13} cm^{-3}. The curves calculated from the proposed model for beryllium (Fig. 1) are very close to those presented in [7]. The deviation is substantial only for low temperatures. The reason for this is that, in our model, the dielectronic recombination rate was calculated with allowance for a larger number of transitions and turned out to be higher in the low-temperature range. The same situation is observed for carbon (Fig. 2) and oxygen (Fig. 3). Good agreement is found for neon (Fig. 4) and argon (Fig. 5), for which the deviations do not exceed 10–15%.

Figures 6–10 illustrate the results of calculating the specific radiation power (per a multielectron ion and per electron) as a function of the temperature with

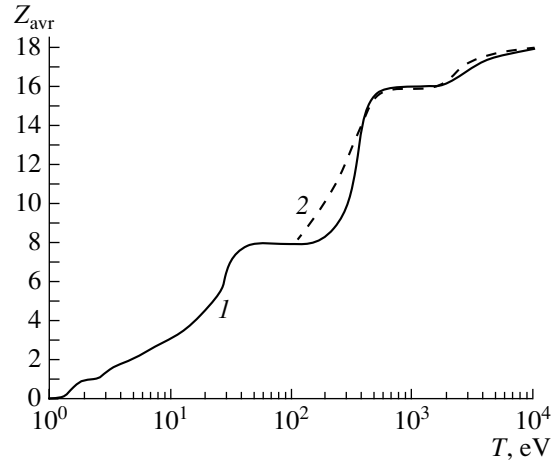

Fig. 5. The same as in Fig. 1, but for argon.

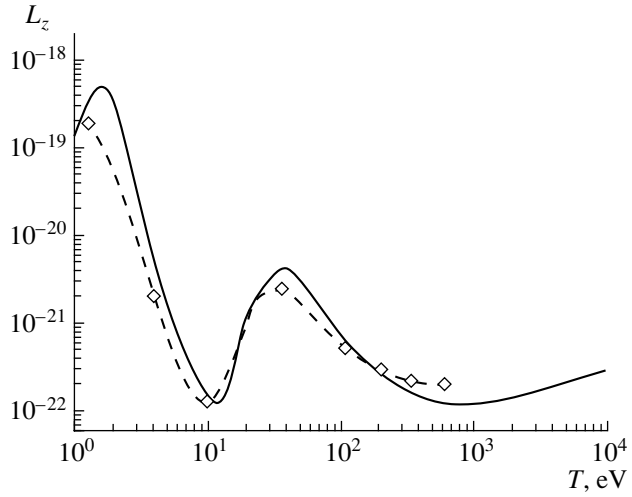

Fig. 6. Specific radiation power from beryllium in a coronal equilibrium (in erg cm@3/s). The solid curve was calculated by the two-group model proposed in the present paper, and the dashed curve was obtained by using the ADPAK computer code [26].

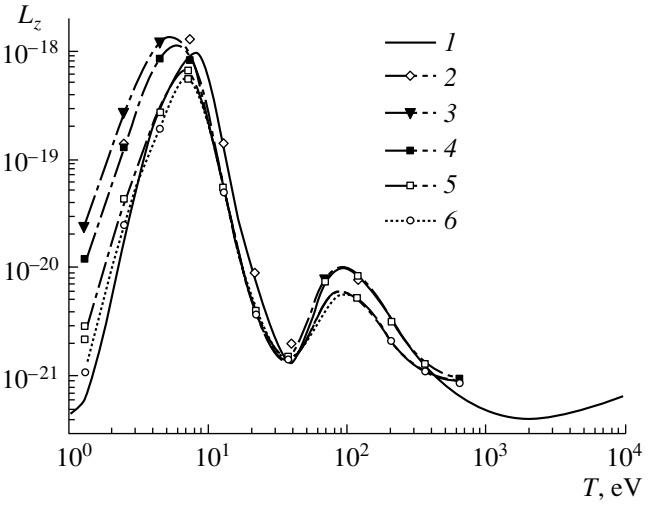

Fig. 7. Specific radiation power from carbon in a coronal equilibrium (in erg cm@3/s). The solid curve was calculated by the two-group model proposed in the present paper, and the dashed curves were obtained from the results of [26].

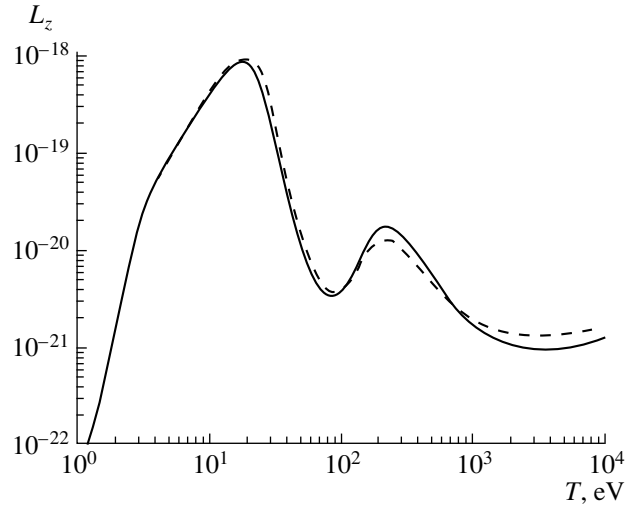

Fig. 8. Specific radiation power from oxygen in a coronal equilibrium (in erg cm^3/s). The solid curve was calculated by the two-group model proposed in the present paper, and the dashed curve was obtained from the results of [7].

allowance for line emission, as well as recombination radiation and bremsstrahlung. In Fig. 6, we compare the results calculated from the two-group model proposed here (solid curve) against the results obtained with the ADPAK code in [26] (dashed curve). In Fig. 7, we compare the specific carbon radiation powers calculated from the two-group model (solid curve) and those obtained from different models in [26]. We can readily see that the agreement of our simplified model with the models used in [26] is no worse than that between the models themselves.

Unfortunately, in [26], there are no data on oxygen. This is why, in Fig. 8, we compared the results of our calculations of the specific oxygen radiation power with those obtained in [7]. Figures 9 and 10 compare the results for neon and argon from the simplified model against the corresponding results of [26]. We recall that all the formulas for calculating radiative losses are rather rough (see, e.g., [7]). In addition, the known accuracy of the rates of elementary processes is low. This is why, even when the results obtained by using different computer codes and different databases

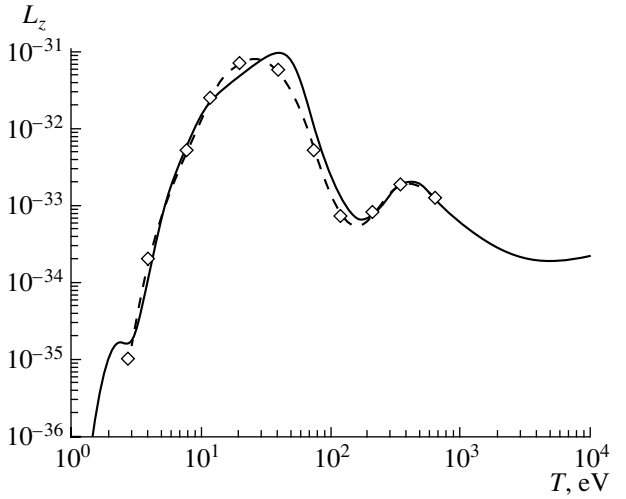

Fig. 9. The same as in Fig. 6, but for neon.

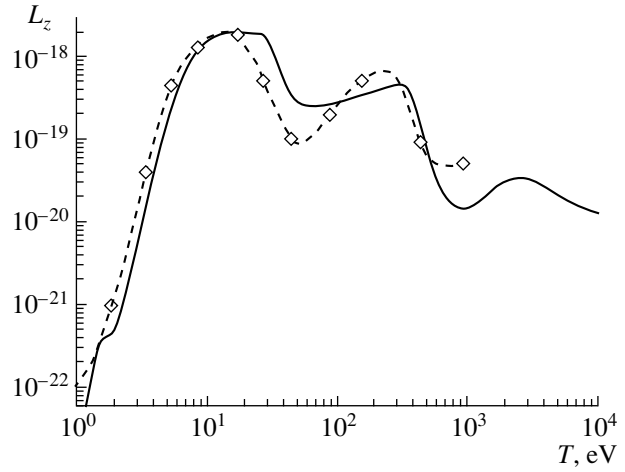

Fig. 10. The same as in Fig. 6, but for argon.

differ by a factor of 1.5–2, the agreement can be considered good. Accordingly, it may be concluded that the simplified model proposed here yields quite correct results.

6. TABLES

Table 1 presents constants for calculating the radiation intensities from estimating formulas in the six-group approximation. The second column shows the spectral index of the element, $I = z + 1$, which is greater than the ion charge number by unity. For each ion, only those transitions are considered for which the oscillator strength exceeds the critical value $f_c = 10^{-2}$. The total number of such transition lines is N_l. The transitions with close energies E_z^{0j} are then combined into groups, i.e., the effective radiation lines, each characterized by its effective transition energy, oscillator strength, lifetime, and initial and final quantum numbers. The number of the group consisting of only one line is marked by an asterisk. The quantity Δ_{err} is the deviation of the radiation power calculated in the six-group approximation with effective lines from the exact radiation power calculated from all N_l lines for which $f_0^{0j} > f_c$ in the electron temperature range 1 eV $\le T_e \le 10^4$ eV. If the values of N_l and Δ_{err} are not given in the table, this means that the emission lines from the corresponding ion are not combined into groups. Metastable lines are ignored, except for those of a neutral carbon atom CI. The metastables can be taken into account with the help of the last raw in the corresponding table. Neutral carbon has four low-lying levels. The energies of two of them are so low that they can be ignored in comparison with the energies that are of practical interest for magnetic fusion systems. The other two levels with the energies $E_1 = 1.264$ eV and $E_2 = 2.684$ eV are important. The radiation power is determined by calculating the power of radiation from the first five lines without allowance for metastable states, by multiplying the result by the relative population of the ground state, equal to $(1 + \exp(-E_1/T) + \exp(-E_2/T))^{-1}$, and then by adding the radiation power calculated from the sixth effective line and multiplied by the relative population of the effective metastable level.

Constants for calculating radiation from formula (4.1) and approximating formulas in the two-group approximation are listed in Table 2. The quantity Δ_{err} is the deviation of the radiation power calculated in the two-group approximation with effective lines from the exact radiation power calculated from all N_l lines for which $f_0^{0j} > f_c$ in the electron temperature range 1 eV $\le T_e \le 10^4$ eV. The exceptions are NeIX, NeX, ArXVII, and ArXVIII ions, for which the approximations are valid in the range 30 eV $\le T_e \le 10^4$ eV.

Finally, Table 3 presents constants for calculating the dielectronic recombination rate from formula (4.2). The last column shows how the calculations from formula (4.2) differ from those with allowance for the six effective transitions in the six-group model. Recall that the bare nucleus cannot be subject to dielectronic recombination.

6. CONCLUSIONS

In this paper, we have presented approximate formulas for calculating the ionization and recombination rates and the rates of emission from individual ions of the chemical elements that are most interesting for tokamak physics, namely, beryllium, carbon, oxygen, neon, and argon. An approximation in which the radiation lines are combined into six groups makes it possible to account for the plasma opacity effects. This is especially important in simulating the injection of pellets and noble gas jets into tokamak plasmas in order to

Table 1. Constants for calculating the radiation intensities from estimating formulas in the six-group approximation

Element	Ion	E^z_{ion}, eV	a_n	Level j	E^{0j}_z, eV	ν^j_z, s^{-1}	f^{0j}_z	n_0	n_1	N_l	Δ_{err}
Be	I	9.323		1*	5.292	5.6×10^8	1.39	2	2	2	
				2*	7.483	1.26×10^7	0.0156	2	3		
Be	II	18.211	0.552	1*	3.969	1.14×10^8	0.501	2	2	4	
				2*	11.995	1.71×10^8	0.0826	2	3		
				3*	14.76	9.82×10^7	0.0313	2	4		
				4*	16.03	5.47×10^7	0.0148	2	5		
Be	III	153.90		1*	124.05	1.23×10^{11}	0.555	1	2	5	
				2*	140.77	3.62×10^{10}	0.127	1	3		
				3*	146.6	1.53×10^{10}	0.0493	1	4		
				4*	149.4	7.80×10^9	0.0243	1	5		
				5*	150.89	4.49×10^9	0.0137	1	6		
Be	IV	217.72		1*	163.7	1.60×10^{11}	0.416	1	2	4	
				2*	194.02	4.28×10^{10}	0.0790	1	3		
				3*	204.64	1.75×10^{10}	0.0290	1	4		
				4*	209.54	8.78×10^9	0.0139	1	5		
C	I	11.26		1*	7.502	3.59×10^8	0.148	2	3	12	0.4%
				2*	7.963	1.17×10^8	0.0714	2	2		
				3*	9.353	2.3×10^8	0.0609	2	2		
				4*	9.734	2.62×10^8	0.107	2	3		
				5	9.857	1×10^8	0.0788	2	3		
				meta	7.1	2.2×10^9	0.35	2	3	5	4%
C	II	24.38	0.095	1*	9.325	2.8×10^8	0.127	2	2	10	3%
				2*	12.00	2.27×10^9	0.122	2	2		
				3*	13.75	4.10×10^9	0.503	2	2		
				4*	18.09	2.85×10^9	0.336	2	3		
				5*	20.89	1.32×10^9	0.117	2	4		
				6	23	5.0×10^8	0.1	2	4		
C	III	47.89	0.56	1*	12.72	1.79×10^9	0.767	2	2	7	2%
				2*	32.20	3.46×10^9	0.232	2	3		
				3*	38.48	9.66×10^8	0.0452	2	4		
				4*	42.7	1.18×10^9	0.0451	2	5		
				5*	44.39	4.65×10^8	0.0164	2	6		
				6*	45.37	3.35×10^8	0.0113	2	7		
C	IV	64.49	0.984	1*	8.025	2.64×10^8	0.285	2	2	5	
				2*	39.79	4.62×10^9	0.203	2	3		
				3*	50.755	2.26×10^9	0.0611	2	4		
				4*	55.79	1.21×10^9	0.0270	2	5		
				5*	58.52	7.15×10^8	0.0145	2	6		
C	V	392.09		1*	308.67	8.89×10^{11}	0.648	1	2	5	
				2*	355.5	2.56×10^{11}	0.141	1	3		
				3*	371.8	1.07×10^{11}	0.0536	1	4		
				4*	379.5	5.41×10^{10}	0.0261	1	5		
				5*	383.6	3.13×10^{10}	0.0148	1	6		
C	VI	490.0		1*	368.4	8.13×10^{11}	0.416	1	2	4	
				2*	436.6	2.17×10^{11}	0.0790	1	3		
				3*	460.5	8.85×10^{10}	0.0290	1	4		
				4*	471.5	4.45×10^{10}	0.0139	1	5		

Table 1. (Contd.)

Element	Ion	E_{ion}^{z}, eV	a_n	Level j	E_z^{0j}, eV	ν_z^j, s^{-1}	f_z^{0j}	n_0	n_1	N_l	Δ_{err}
O	I	13.618		1*	9.536	5.92×10^8	0.0503	2	3	7	0.5%
				2	12.45	6.8×10^7	0.035	2	4		
				3*	12.56	2.19×10^8	0.0535	2	3		
				4*	14.15	6.78×10^8	0.0784	2	3		
				5*	15.69	6.58×10^8	0.0619	2	2		
				6*	16.15	2.14×10^8	0.0190	2	4		
O	II	35.118	0.507	1*	14.91	8.51×10^8	0.266	2	2	6	
				2*	23.04	9.94×10^8	0.130	2	3		
				3*	28.9	4.46×10^9	0.371	2	3		
				4*	29.68	1.85×10^8	0.0146	2	4		
				5*	31.71	2.37×10^9	0.164	2	4		
				6*	33.0	1.37×10^9	0.0872	2	5		
O	III	54.936	0.658	1*	14.90	6.15×10^8	0.107	2	2	14	0.3%
				2*	17.67	18.5×10^8	0.137	2	2		
				3*	24.47	1.43×10^{10}	0.185	2	2		
				4*	33.23	39.6×10^8	0.0831	2	3		
				5	40.66	2×10^{10}	0.630	2	3		
				6	48.0	6×10^9	0.44	2	4		
O	IV	77.414	0.718	1*	15.75	7.07×10^8	0.110	2	2	16	0.1%
				2*	22.0	6×10^9	0.40	2	2		
				3*	44.39	8.02×10^9	0.314	2	2		
				4*	52.12	3.55×10^{10}	0.504	2	3		
				5	61.0	1.1×10^{10}	0.337	2	3		
				6	71.0	4×10^{10}	0.18	2	4		
O	V	113.90	0.735	1*	19.74	2.89×10^9	0.515	2	2	8	0.02%
				2*	72.18	2.96×10^{10}	0.395	2	3		
				3*	89.42	6.66×10^9	0.0579	2	3		
				4*	91.73	9.41×10^9	0.0777	2	4		
				5*	99.76	7.16×10^9	0.050	2	5		
				6	106.0	4×10^9	0.0505	2	7		
O	VI	138.12	1.07	1*	12.021	4.14×10^8	0.199	2	2	6	
				2*	82.81	2.62×10^{10}	0.265	2	3		
				3*	107.34	1.23×10^{10}	0.0741	2	4		
				4*	118.6	6.48×10^9	0.0320	2	5		
				5*	124.7	3.78×10^9	0.0169	2	6		
				6*	128.4	2.39×10^9	0.0101	2	7		
O	VII	736.34		1*	575.5	3.32×10^{12}	0.696	1	2	5	
				2*	668.3	9.35×10^{11}	0.146	1	3		
				3*	698.3	3.89×10^{11}	0.0552	1	4		
				4*	714.4	1.97×10^{11}	0.0268	1	5		
				5*	722.7	1.13×10^{11}	0.0151	1	6		
O	VIII	871.417		1*	655.2	2.57×10^{12}	0.416	1	2		
				2*	776.9	6.86×10^{11}	0.0790	1	3		
				3*	817.8	2.80×10^{11}	0.0290	1	4		
				4*	839.9	1.41×10^{11}	0.0139	1	5		

Table 1. (Contd.)

Element	Ion	E_{ion}^{z}, eV	a_n	Level j	E_z^{0j}, eV	ν_z^j, s^{-1}	f_z^{0j}	n_0	n_1	N_l	Δ_{err}
Ne	I	21.565		1*	16.713	4.86×10^7	0.0121	2	3	4	
				2*	16.89	3.12×10^8	0.149	2	3		
				3*	19.83	7.41×10^7	0.0131	2	4		
				4*	20.091	9.29×10^7	0.016	2	3		
Ne	II	40.963	0.289	1*	26.9	8.05×10^9	0.0856	2	2	14	0.12%
				2*	27.96	3.88×10^9	0.116	2	3		
				3*	30.6	1.58×10^9	0.0651	2	3		
				4	34.88	2.1×10^9	0.165	2	3		
				5	37.83	2.2×10^9	0.158	2	3		
				6*	39.0	1.8×10^9	0.0553	2	5		
Ne	III	63.46	0.596	1*	25.39	4.87×10^9	0.175	2	2	15	3%
				2*	39.62	1.11×10^{10}	0.0546	2	3		
				3	44.25	4×10^9	0.112	2	3		
				4	49.52	1×10^{10}	0.186	2	3		
				5	54.66	1×10^{10}	0.355	2	3		
				6	57.22	7×10^9	0.213	2	4		
Ne	IV	97.12	0.0742	1*	22.9	1.76×10^9	0.233	2	2	5	
				2*	59.59	6.74×10^{10}	0.132	2	3		
				3*	72.02	6.92×10^{10}	0.927	2	3		
				4*	78.82	4.07×10^9	0.0455	2	4		
				5*	83.54	2.90×10^{10}	0.289	2	4		
Ne	V	126.2	0.789	1	22.55	2.1×10^9	0.178	2	2	15	12%
				2	34.9	2.0×10^{10}	0.160	2	2		
				3	86.86	1×10^{11}	0.92	2	3		
				4	94.53	2×10^{10}	0.173	2	3		
				5	105.1	2×10^{10}	0.325	2	4		
Ne	VI	157.9	0.787	1*	22.14	1.15×10^9	0.175	2	2	14	7%
				2	30.0	1×10^{10}	0.0546	2	2		
				3	106.8	1.0×10^{11}	0.112	2	3		
				4	122.6	1×10^{10}	0.186	2	3		
				5*	126.6	5×10^{10}	0.355	2	4		
				6	138.9	2.2×10^{10}	0.213	2	4		
Ne	VII	207.28	0.793	1*	26.72	4.00×10^9	0.389	2	2	5	
				2*	127.5	1.14×10^{11}	0.486	2	3		
				3*	151.6	1.20×10^{10}	0.0364	2	3		
				4*	164.0	4.88×10^{10}	0.126	2	4		
				5*	179.4	5.42×10^9	0.0117	2	4		
Ne	VIII	239.1	1.107	1*	16.07	5.68×10^8	0.153	2	2	6	
				2*	141.09	8.65×10^{10}	0.302	2	3		
				3*	184.5	3.98×10^{10}	0.0812	2	4		
				4*	204.4	2.08×10^{10}	0.0345	2	5		
				5*	215.3	1.21×10^{10}	0.0181	2	6		
				6*	221.8	7.65×10^9	0.0108	2	7		

Table 1. (Contd.)

Element	Ion	E_{ion}^{z}, eV	a_n	Level j	E_z^{0j}, eV	ν_z^j, s^{-1}	f_z^{0j}	n_0	n_1	N_l	Δ_{err}
Ne	IX	1195.84		1*	924.85	8.09×10^{12}	0.724	1	2	5	
				2*	1076	2.48×10^{12}	0.149	1	3		
				3*	1130	1.03×10^{12}	0.0561	1	4		
				4*	1155	5.20×10^{11}	0.0271	1	5		
				5*	1168	3.00×10^{11}	0.0153	1	6		
Ne	X	1362.21		1*	1025	6.28×10^{12}	0.416	1	2	4	
				2*	1214	1.68×10^{12}	0.0790	1	3		
				3*	1280	6.84×10^{11}	0.0290	1	4		
				4*	1311	3.44×10^{11}	0.0139	1	5		
Ar	I	15.76		1*	11.65	1.3×10^{8}	0.0665	3	4	6	
				2*	11.86	4.94×10^{8}	0.244	3	4		
				3*	14.14	7.70×10^{7}	0.0268	3	5		
				4*	14.19	2.69×10^{8}	0.0930	3	3		
				5*	14.30	3.5×10^{7}	0.0119	3	5		
				6*	14.35	3.14×10^{8}	0.106	3	3		
Ar	II	27.63	0.1154	1*	13.45	4.22×10^{8}	0.018	3	3	19	1.6%
				2*	17.17	2.76×10^{9}	0.217	3	4		
				3	19.0	2.3×10^{9}	0.241	3	4		
				4	21.5	6.4×10^{9}	0.855	3	3		
				5	23.7	4×10^{9}	0.669	3	5		
				6	25.7	3.3×10^{9}	0.95	3	5		
Ar	III	40.91	0.42	1*	14.14	3.32×10^{8}	0.0385	3	3	16	8%
				2	23.0	4×10^{9}	0.31	3	4		
				3*	25.37	2.15×10^{10}	0.258	3	3		
				4*	25.74	2.56×10^{10}	0.897	3	4		
				5	26.3	3×10^{10}	2.1	3	3		
Ar	IV	59.81	0.532	1*	14.68	2.40×10^{8}	0.0774	3	3	3	
				2*	27.50	3.38×10^{10}	3.11	3	3		
				3*	31.23	1.71×10^{9}	0.122	3	4		
Ar	V	75	0.612	1*	14.96	2.48×10^{8}	0.0428	3	3	6	
				2*	17.46	7.98×10^{8}	0.0607	3	3		
				3*	23.63	2.19×10^{10}	0.302	3	3		
				4*	26.9	1.8×10^{10}	0.574	3	3		
				5*	27.75	2.77×10^{10}	1.39	3	3		
				6*	36.78	8.28×10^{9}	0.142	3	4		
Ar	VI	91.01	0.626	1*	16.29	4.54×10^{8}	0.0661	3	3	7	0.4%
				2*	20.93	4.90×10^{9}	0.0865	3	3		
				3*	22.56	1.43×10^{10}	0.648	3	3		
				4*	27.02	1.77×10^{10}	0.936	3	3		
				5*	42.42	1.92×10^{10}	0.0824	3	4		
				6	56.5	4×10^{10}	0.078	3	4		
Ar	VII	124.32	0.655	1*	21.21	8.04×10^{9}	1.24	3	3	2	
				2*	70.23	1.28×10^{10}	0.179	3	4		
Ar	VIII	143.4	0.62	1*	17.66	2.57×10^{9}	0.573	3	3	3	
				2*	78.18	1.09×10^{10}	0.124	3	4		
				3*	103.6	6.75×10^{9}	0.0438	3	5		

Table 1. (Contd.)

Element	Ion	E_{ion}^{z}, eV	a_n	Level j	E_z^{0j}, eV	ν_z^j, s^{-1}	f_z^{0j}	n_0	n_1	N_l	Δ_{err}
Ar	IX	422.4		1*	255.2	2.23×10^{11}	0.238	3	4	7	1.5%
				2*	300.0	2.60×10^{12}	2.01	3	4		
				3*	347.2	5.77×10^{11}	0.333	3	4		
				4*	355.1	2.50×10^{11}	0.524	3	5		
				5*	380.1	5.79×10^{11}	0.278	3	7		
				6*	394.6	3.43×10^{11}	0.153	3	8		
Ar	X	478.7	0.788	1*	74.34	4.75×10^{10}	0.0663	2	2	14	1%
				2	323.7	2.5×10^{11}	0.458	2	3		
				3	330.2	2×10^{12}	1.7	2	3		
				4	339.6	4.5×10^{11}	0.10	2	3		
Ar	XI	539.0	0.815	1*	65.77	2.15×10^{10}	0.115	1	2	7	0.1%
				2*	321.2	1.78×10^{11}	0.0665	2	3		
				3*	350.1	8.07×10^{11}	0.254	2	3		
				4	365	2×10^{12}	1.381	2	3		
Ar	XII	618.3	0.828	1*	56.24	6.62×10^{9}	0.145	2	2	5	
				2*	358.2	2.03×10^{11}	0.11	2	3		
				3*	396.0	3.93×10^{12}	1.74	2	3		
				4*	406.2	5.82×10^{11}	0.245	2	3		
				5*	497.2	1.35×10^{12}	0.382	2	4		
Ar	XIII	686.3	0.876	1*	50.74	3.72×10^{9}	0.0558	2	2	10	0.8%
				2*	59.76	9.6×10^{9}	0.062	2	2		
				3*	76.26	5.4×10^{10}	0.0718	2	2		
				4	422	4×10^{12}	1.58	2	3		
Ar	XIV	755.7	0.85	1*	49.13	3.24×10^{9}	0.0517	2	2		
				2*	66.83	2.53×10^{10}	0.132	2	2		
				3*	450.4	3.43×10^{12}	0.652	2	3		
				4*	487.5	1.57×10^{12}	0.153	2	3		
				5*	589.1	1.13×10^{12}	0.126	2	4		
Ar	XV	854.8	0.86	1*	56.24	9.32×10^{9}	0.205	2	2		
				2*	503.2	2.31×10^{12}	0.636	2	3		
				3*	661.2	1.47×10^{11}	0.0331	2	3		
				4*	661.2	1.04×10^{12}	0.166	2	4		
Ar	XVI	918.0	1.157		34.06	1.41×10^{9}	0.0842	2	2		
Ar	XVII	4120		1*	3147	1.11×10^{14}	0.775	1	2		
				2*	3688	3.04×10^{13}	0.155	1	3		
				3*	3884	1.24×10^{13}	0.0573	1	4		
				4*	3974	6.27×10^{12}	0.0276	1	4		
				5*	4016	3.60×10^{12}	0.0155	1	5		
Ar	XVIII	4426		1*	3332	6.64×10^{13}	0.416	1	2		
				2*	3946	1.77×10^{13}	0.0790	1	3		
				3*	4157	7.22×10^{12}	0.0290	1	4		
				4*	4257	3.63×10^{12}	0.0139	1	5		

Table 2. Constants for calculating radiation from formula (4.1) and approximating formulas in the two-group approximation

Element	Ion	C_1^{rad}	C_2^{rad}	E_1^{rad}	E_1^{rad}	λ	Δ_{err}
Be	I	3.55	7.1	6	31	0.3	12%
Be	II	7.3	0	3.85	0	0.315	8%
Be	III	1.57	0	123.4	0	0.315	8%
Be	IV	1.2	0	163	0	0.25	10%
C	I	1.3	1.66	7.7	18	0.28	8%
With allowance for metastables	I	1.3	0	7.3	0	0.265	10%
C	II	0.78	5.51	10	18	0.25	8%
C	III	9.1	9.1×10^{-8}	12.5	0	0.3	8%
C	IV	8.47×10^{-6}	5.65	0	7.8	0.315	6%
C	V	1.9	0	308.2	0	0.27	14%
C	VI	1.18	0	367.9	0	0.27	17%
O	I	0.55	1.15	10.0	20.0	0.3	8%
O	II	3.37	3.20	14.6	29.0	0.295	5%
O	III	2.15	4.5	15.0	28.0	0.25	7%
O	IV	2.8	5.5	16.1	35.0	0.27	15%
O	V	6.2	0	19.3	0	0.27	8%
O	VI	2.66	0.865	11.7	100	0.29	7%
O	VII	1.76	0	574.7	0	0.26	17%
O	VIII	1.05	0	654.4	0	0.27	18%
Ne	I	0.635	0	16.6	0	0.22	9%
Ne	II	0.50	1.2	26.4	32.0	0.22	16%
Ne	III	1.7	1.9	24.9	47.0	0.24	10%
Ne	IV	2.38	1.1	22.3	83.0	0.19	9%
Ne	V	2.12	3.5	21.9	60	0.23	10%
Ne	VI	1.7	3.5	22.0	42	0.23	16%
Ne	VII	5.0	0.15	26.4	140	0.28	14%
Ne	VIII	2.62	0	15.7	0	0.27	15%
Ne	IX	0.935	0	916.7	0	0.2	12%
Ne	X	0.63	0	1018	0	0.23	11%
Ar	I	1.4	0	11.6	0	0.18	16%
Ar	II	0.48	9.0	15.0	22.4	0.22	10%
Ar	III	0.207	18	13.5	24	0.25	12%
Ar	IV	8	8	14.0	25.5	0.18	8%
Ar	V	0.61	22.1	14.7	24.6	0.3	9%
Ar	VI	1.1	6.8	17.6	30.0	0.26	20%
Ar	VII	16.0	0	21.0	0	0.33	6%
Ar	VIII	12.0	0	17.4	0	0.32	5%
Ar	IX	0.62	3.0	254.5	301	0.16	12%
Ar	X	0.163	3.5	72.6	360	0.2	15%
Ar	XI	2.0	11.5	65.6	480	0.4	18%
Ar	XII	1.65	5.5	55.5	500	0.29	16%
Ar	XIII	0.8	0.78	50.7	300	0.13	12%
Ar	XIV	0.639	0	48.6	0	0.07	18%
Ar	XV	3.0	2.6	55.8	700	0.345	10%
Ar	XVI	1.95	0	33.85	0	0.39	6%
Ar	XVII	0.67	0	3124	0	0.2	15%
Ar	XVIII	0.365	0	3305	0	0.2	14%

Table 3. Constants for calculating the dielectronic recombination rate from formula (4.2)

Element	Ion	α	β_1	β_1	C_z^1	C_z^2	$E_{dr}^{(1)}$	$E_{dr}^{(2)}$	Δ_{err}
Be	II	1.33	0.14	0.32	0.0145	0.016	3.7	14.0	8%
Be	III	1.43	0.19	0.045	1.85	0.278	124	160	25%
Be	IV	1.5	0.12	0.07	5.1	2.55	164	220	20%
C	II	1.407	0.14	0.25	9.25×10^{-3}	2.5	8.3	23	15%
C	III	1.48	0.117	0.0095	1.6	1.6	13	40	8%
C	IV	1.48	0.11	0.01	1.07	2.9	8.1	40	8%
C	V	1.451	0.002	0	11.8	0	308.5	0	8%
C	VI	1.467	0.001	0	1.275	0	368.4	0	4%
O	II	1.375	0.142	0.265	0.02	0.148	15.0	29.0	12%
O	III	1.453	0.15	0.165	0.136	3.6	17.0	44.0	25%
O	IV	1.41	0.135	0	0.453	0	18.5	0	9%
O	V	1.49	0.14	0.05	1.22	8.5	19.1	70.0	19%
O	VI	1.49	0.14	0.03	0.644	9.90	11.55	82.0	12%
O	VII	1.44	0.014	0	22.13	0	540	0	11%
O	VIII	1.46	0.013	0	20.4	0	607	0	8%
Ne	II	1.34	0.26	0	0.0448	0	16.7	0	13%
Ne	III	1.44	0.185	0.16	0.47	1	28.1	37	25%
Ne	IV	1.48	0.15	0.10	0.294	15.4	23.0	76	23%
Ne	V	1.47	0.15	0.053	0.67	23.0	24.5	87	18%
Ne	VI	1.49	0.14	0.03	1.7	34	27	110	12%
Ne	VII	1.49	0.13	0.019	2.85	29.6	27	132	8%
Ne	VIII	1.49	0.13	0.01	1.23	26.0	16.5	150	7%
Ne	IX	1.49	0.005	0	51	0	945	0	5%
Ne	X	1.475	0.004	0	31.5	0	1035	0	3%
Ar	II	1.34	0.26	0	0.343	0	20.4	0	8
Ar	III	1.42	0.175	0	3.6	0	24.5	0	20
Ar	IV	1.42	0.12	0	3.55	0	26.0	0	18
Ar	V	1.42	0.12	0	6.2	0	27.2	0	16
Ar	VI	1.42	0.12	0	7.0	0	24.1	0	20
Ar	VII	1.46	0.132	0.025	7.05	6.34	21.2	65	5
Ar	VIII	1.48	0.132	0.014	4.6	9.2	17.7	88.0	8
Ar	IX	1.5	0.006	0	330	0	303	0	15
Ar	X	1.5	0.13	0.003	250	250	73.3	330	7
Ar	XI	1.46	0.125	0.0029	3.5	177.8	66	340	8
Ar	XII	1.48	0.126	0.0022	4.65	320.1	57.0	390	4
Ar	XIII	1.43	0.13	0.004	6.52	163	57	380	10
Ar	XIV	1.44	0.125	0.0055	8.125	125	57	430	8
Ar	XV	1.45	0.12	0.001	12.28	132	57	500	6
Ar	XVI	1.445	0.1	0	4.43	0	34.06	0	5
Ar	XVII	1.5	0	0	125	0	3170	0	7
Ar	XVIII	1.5	0	0	82	0	3500	0	6

reduce the consequences of major disruptions and also in simulating the current decay process and the generation of runaway electrons during a major disruption. We have given all the constants required for calculations.

We have also written out the simplest approximating formulas for radiation from ions in a given ionization state in an optically thin plasma. The results of calculations from these formulas differ from the results of exact calculations (those that account for all the emission lines for which the relative oscillator strengths exceed 10^{-2}) by at most 25%. Such an accuracy can be regarded as quite satisfactory in view of the fact that the results of present-day simulations utilizing different databases can differ by a factor of 2 or more. We have compared our results with the widely known results calculated in the coronal equilibrium approximation and have found that they are in satisfactory agreement. Hence, the proposed approximating formulas can be successfully applied to an optically thin plasma.

For an optically thick plasma, the approximating formulas provide at least qualitative estimates of the opacity effects, which may play a dominant role in some tokamak operating modes. In [6], it was shown that the results obtained with allowance for the opacity effects by the method used in the present paper agree qualitatively with the experimental data for carbon. However, in order to draw final conclusions about the accuracy of the methods proposed here for calculating radiative losses from an optically thick plasma, it is necessary to carry out rather involved calculations with the use of the Biberman–Holstein equation.

ACKNOWLEDGMENTS

We are grateful to K.M. Lobanov and A.B. Mineev (Efremov Research Institute of Electrophysical Apparatus, St. Petersburg, Russia) for carefully reading the paper and giving valuable remarks. This work was supported in part by the Department of Atomic Science and Technology of the RF Ministry of Atomic Industry.

APPENDIX

List of Notation

The notations used in the present paper are as follows:

z is the ion charge number;

Z is the atomic number of the element;

T_e is the electron temperature;

n_z is the density of the ions with the charge number z;

n_e is the electron density;

Q_z is the total radiation intensity from the ions with the charge number z;

$L_z(T_e)$ is the radiation intensity from the ions with the charge number z, divided by the electron density and the density of the ions with the charge number z;

E_z^{jk} is the energy of transition between the j th and kth states;

E_{ion}^{jk} is the minimum ionization energy of an ion with a charge number z;

f_z^{jk} is the oscillator strength for the transition;

n_0 is the principal quantum number of the ground state;

n_1 is the principal quantum number of the excited state;

a_n is the numerical factor given in the tables;

$E_1(x) = \int_x^\infty \frac{\exp(-t)dt}{t}$ is the exponential integral;

κ_z^j is the reciprocal of the mean distance that a resonant photon travels before being absorbed;

ρ is the characteristic dimension of a cloud of ions of a given species;

β_z^j is the ratio of the electron-impact quenching probability to the radiative decay probability;

W_z^j is a function accounting for the attenuation of a given emission line as it escapes from a plane cloud (of thickness ρ) of ions with the charge number z;

T_a is the probability for a photon to travel a distance ρ without being absorbed;

λ_z^j is the wavelength of a photon;

Γ/γ is the ratio between the observed and natural (radiative) line widths;

ν_z^j is the reciprocal of the natural radiative decay time of an excited state;

m_p is the mass of a proton;

M is the mass of an impurity ion;

$I_{z\text{ground}}$ is the ionization rate from the ground state;

$I_{z\text{ex}}$ is the ionization rate from the excited state;

R_{3b}^z is the three-body recombination rate;

R_{photo}^z is the photorecombination rate;

R_{dial}^z is the dielectronic recombination rate;

$C_{1,2}^{\text{rad}}$, $E_{1,2}^{\text{rad}}$, and λ are parameters in the approximating formula for radiation from an impurity ion;

the functions B_z (dependent on the charge of a recombining ion), A_{zj} (dependent on the charge, transition energy, and oscillator strength), and D_{zj} and n_t (both dependent on the temperature, charge, and electron density) determine the dielectronic recombination rate;

$C_z^{1,2}$ and $E_{\text{dr}}^{1,2}$ are parameters in the approximating formula for the dielectronic recombination rate;

R_z^{cx} is the rate of charge exchange between an ion
1 wirh a charge number z and hydrogen atoms;

σ_z^{cx} is the cross section for charge exchange between an ion with a charge number z and hydrogen atoms;

v_n is the velocity of a hydrogen atom;

E_n is the kinetic energy of a hydrogen atom; and

the asterisk in the symbols like 1* indicates the numbers of the groups containing only one radiation line.

REFERENCES

1. G. R. Harris, Preprint no. JET-R (90) 07 (JET Joint Undertaking, Abingdon, 1990).
2. D. G. Whyte, T. C. Jernigan, D. A. Humphreys, et al., J. Nucl. Mater. **313–316**, 1239 (2003).
3. E. M. Hollmann, T. C. Jernigan, D. G. Groth, et al., in *Proceedings of the 20th International Conference on Fusion Energy, Viena, 2004*, CD-ROM file EX/10-6Ra.
4. M. Bakhtiari, Y. Kawano, H. Tamai, et al., in *Proceedings of the 20th International Conference on Fusion Energy, Viena, 2004,* CD-ROM file EX/10-6Rb.
5. G. Martin, F. Sourd, F. Saint-Laurent, et al., in *Proceedings of the 20th International Conference on Fusion Energy, Viena, 2004*, CD-ROM file EX/10-6Rc.
6. D. Kh. Morozov, V. I. Gervids, I. Yu. Senichenkov, et al., Nucl. Fusion **44**, 252 (2004).
7. D. E. Post, R. V. Jensen, C. B. Tarter, et al., At. Data Nucl. Data Tables **20**, 397 (1977).
8. V. I. Gervids, V. P. Zhdanov, V. I. Kogan, et al., in *Reviews of Plasma Physics*, Ed. by M. A. Leontovich and B. B. Kadomtsev (Atomizdat, Moscow, 1982; Consultants Bureau, New York, 1986), Vol. 12.
9. V. I. Gervids, A. G. Zhidkov, V. S. Marchenko, and S. I. Yakovlenko, in *Reviews of Plasma Physics*, Ed. by M. A. Leontovich and B. B. Kadomtsev (Atomizdat, Moscow, 1982; Consultants Bureau, New York, 1986), Vol. 12.
10. J. D. Huba, *NRL Plasma Formulary* (Naval Research Laboratory, Washington, 2000).
11. V. A. Bazylev and M. I. Chibisov, in *Reviews of Plasma Physics*, Ed. by M. A. Leontovich and B. B. Kadomtsev (Atomizdat, Moscow, 1982; Consultants Bureau, New York, 1986), Vol. 12.
12. U. I. Safronova and V. S. Senashenko, in *Reviews of Plasma Physics*, Ed. by M. A. Leontovich and B. B. Kadomtsev (Atomizdat, Moscow, 1982; Consultants Bureau, New York, 1986), Vol. 12.
13. V. A. Bazylev and M. I. Chibisov, Opt. Spektrosk. **50**, 833 (1981) [Opt. Spectrosc. **50**, 457 (1981)].
14. V. A. Abramov, V. I. Kogan, and V. S. Lisitsa, in *Reviews of Plasma Physics,* Ed. by M. A. Leontovich and B. B. Kadomtsev (Atomizdat, Moscow, 1982; Consultants Bureau, New York, 1986), Vol. 12.
15. V. I. Kogan, in *Encyclopedia of Low-Temperature Plasma*, Ed. by V. E. Fortov (Nauka, Moscow, 2000), Vol. 1, p. 481 [in Russian].
16. A. V. Eletskiĭ and B. M. Smirnov, in *Encyclopedia of Low-Temperature Plasma*, Ed. by V. E. Fortov (Nauka, Moscow, 2000), Vol. 1, p. 219 [in Russian].
17. V. Rozhansky, I. Senichenkov, I. Veselova, et al., Nucl. Fusion **46**, 367 (2006).
18. O. P. Zhdanov, in *Reviews of Plasma Physics,* Ed. by M. A. Leontovich and B. B. Kadomtsev (Atomizdat, Moscow, 1982; Consultants Bureau, New York, 1986), Vol. 12.
19. V. A. Abramov, F. F. Baryshnikov, A. I. Kazanskiĭ, et al., in *Reviews of Plasma Physics*, Ed. by M. A. Leontovich and B. B. Kadomtsev (Atomizdat, Moscow, 1982; Consultants Bureau, New York, 1986), Vol. 12.
20. M. I. Chibisov, Preprint No. 3233 (Kurchatov Institute, Moscow, 1980).
21. R. A. Phaneuf, R. K. Janev, and H. T. Hunter, Nucl. Fusion, Special Suppl., 7 (1987).
22. V. A. Abramov, V. S. Lisitsa, and A. Yu. Pigarov, Pis'ma Zh.Éksp. Teor. Fiz. **42**, 288 (1985) [JETP Lett. **42**, 283 (1985)].
23. F. B. Rosmej, D. Reiter, V. S. Lisitsa, et al., Plasma Phys. Controlled Fusion **41**, 191 (1999).
24. V. I. Kogan, V. I. Gervids, and D. Kh. Morozov, Fiz. Plazmy **27**, 994 (2001) [Plasma Phys. Rep. **27**, 938 (2001)].
25. D. A. Verner, E. M. Verner, and G. J. Ferland, At. Data Nucl. Data Tables **64**, 1 (1996).
26. D. E. Post, J. Nucl. Mater. **220**, 143 (1995).

Translated by O.E. Khadin

SPELL: 1. wirh

View publication stats